Monitoring of Stress Changes using Direct and Coda Wave Velocity Measurements in Faulted and Intact Granite Samples

K. Pandey[1], T. Taira[2], G. Dresen[3] and T. H. Goebel[1] (1: University of Memphis, 2:Berkeley Seismological Laboratory; 3 German Research Centre for Geosciences GFZ)

Summary

- A better understanding of damage accumulation before dynamic failure events in geological material is essential to improve seismic hazard assessment. Previous research has demonstrated the sensitivity of seismic velocities to variations in crack geometry, with established evidence indicating that initial crack closure induces rapid changes in velocity. Our study extends these findings by investigating velocity changes by applying coda wave interferometry (CWI).
- We use an array of 16 piezoceramic transducers to send and record ultrasonic pulses and to determine changes in seismic velocity on intact and faulted Westerly granite samples. Velocity changes are determined from CWI and direct phase arrivals.
- Seismic velocities demonstrate higher sensitivity to damage accumulation under increasing differential stress than macroscopic measurements. Axial stress measured by an external load cell deviates from linearity around two-third through the experiment at a stress level of 290 MPa higher than during the initial drop in seismic velocities.
- Direct waves exhibit strong anisotropy with increasing differential stress and accumulating damage before rock fracture. Coda waves, on the other hand, effectively average over elastic wave propagation for both fast and slow directions, and the resulting velocity estimates show little evidence for anisotropy.
- The results demonstrate the sensitivity of seismic velocity to damage evolution at various boundary conditions and progressive microcrack generation with long lead times before dynamic fracture.

Triaxial Experiment Setup

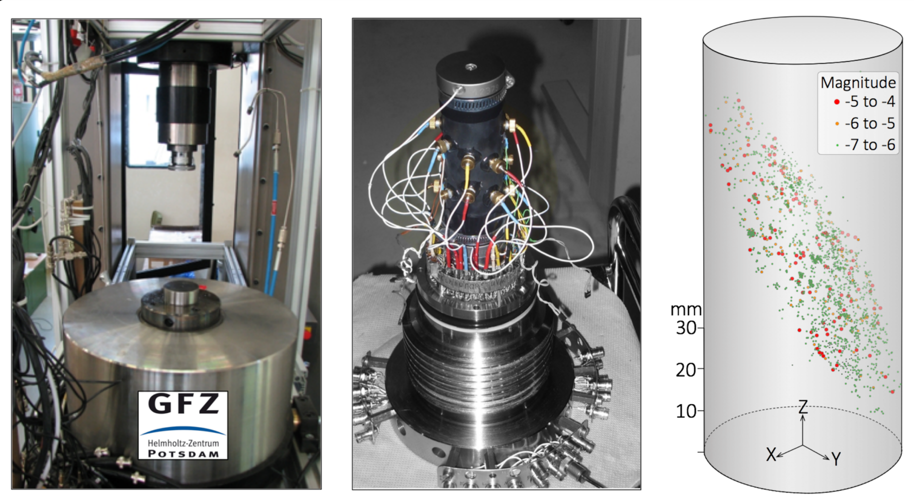

- This study focuses on seismic velocity changes with increasing confining pressures and axial load before rock fracture in cylindrical Westerly granite samples (40–50 mm in diameter and 105 mm in height).
- The samples are comprised of quartz (28 per cent), plagioclase feldspar (33 per cent), orthoclase feldspar (33 per cent) and mica (5 per cent), including muscovite and biotite.

Figure 1: Laboratory set-up (left), sample with acoustic emission sensors (center) and example of acoustic emission location and magnitudes during a stick-slip test (right). The rock mechanics laboratory at GFZ-Potsdam includes a triaxial loading rig with separate pore pressure system and advanced instrumentation for mechanical, hydraulic and seismic data.

Array of Piezoceramic Transducer

- A total of 16 transducers were used, with seven transducer pairs in horizontal alignment and one pair in a vertical arrangement.

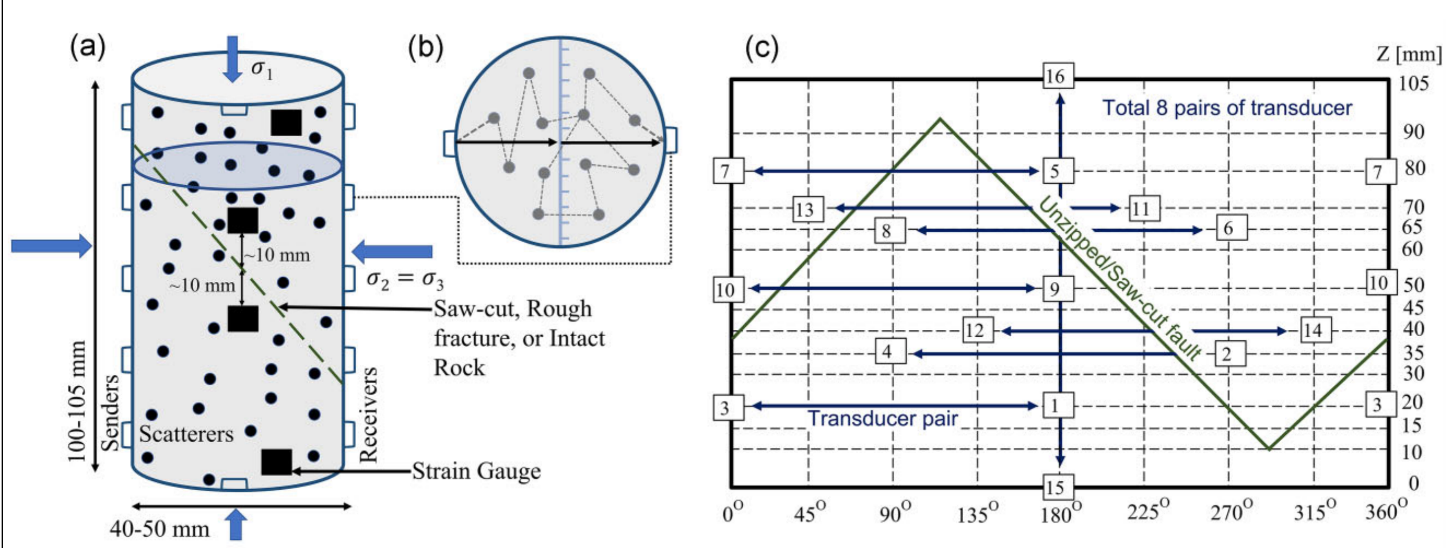

Figure 2: (a) Schematic diagram representing the state of stress (σ1, σ2 and σ3 represent the largest compressive stress, intermediate stress, and least principal stress, respectively), saw-cut fault (blue dashed line) for faulted sample, and scatterers in the rock sample. Sample lengths varied between 100 and 105 mm, and diameter was either 40 or 50 mm. In an active source experiment with sender and receiver pairs, the piezoceramic transducers were directly attached to the rock surface through the rubber jacket. On the sample were two sets of strain gauges, one running circumferentially and the other running axially (black square box). (b) Plan-sectional view of the rock cylinder along its diameter. The solid black lines denote the direct ray path, and the dashed black lines represent the multiply scattered elastic waves from the sender towards the receiver during an experiment. (c) Location of sensors on the rock sample during the experiment and mapping for saw-cut and fractured samples in green.

Coda Wave Interferometry (CWI)

Temporal Variations in Seismic Wavefield

- Laboratory seismograms show the compression and stretching pattern due to variations in confining pressure applied to the rock sample.

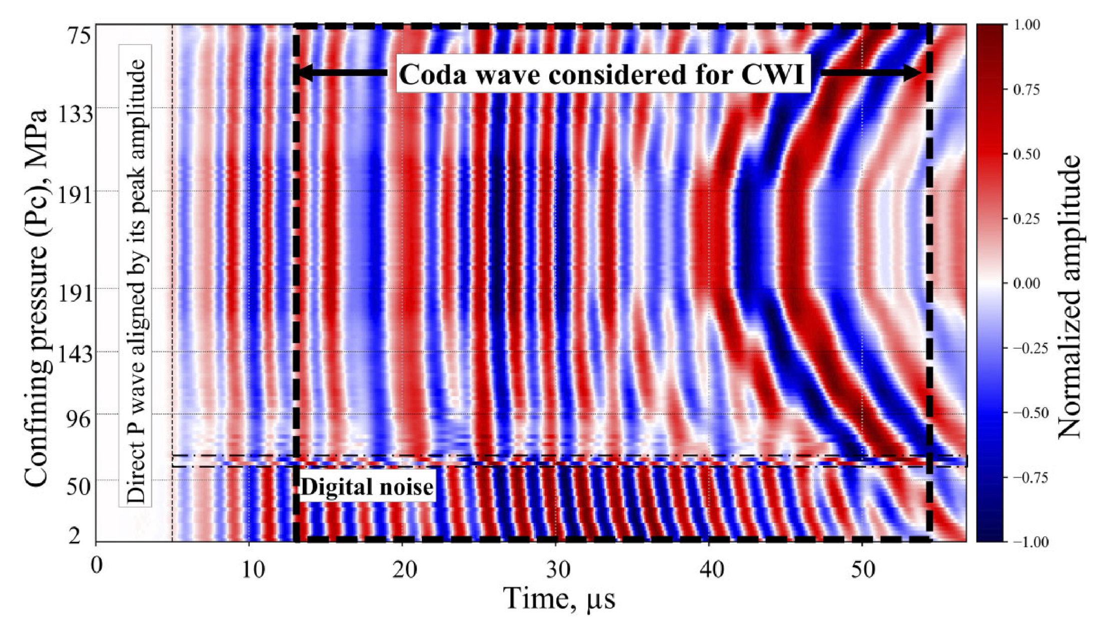

Figure 3: Confining pressure change versus the waveforms recorded during the Int-2 experiment for Sender-4 and Receiver-2 pair. All the waveforms were normalized by the maximum amplitude of the overall recorded waveforms. The P arrivals were used to align the normalized waveforms where the P phase was picked using the AIC picker. The confining pressure was increased from 2 to 191 MPa, then held constant at 191 MPa for 120 min and it lowered to 75 MPa. We observe some digital noise between 60 and 70 MPa, but the recordings are otherwise highly coherent. The red shades of color represent the positive amplitude and the blue shades of color represent the negative amplitude. The black dashed box shows the length of the coda wave used for CWI.

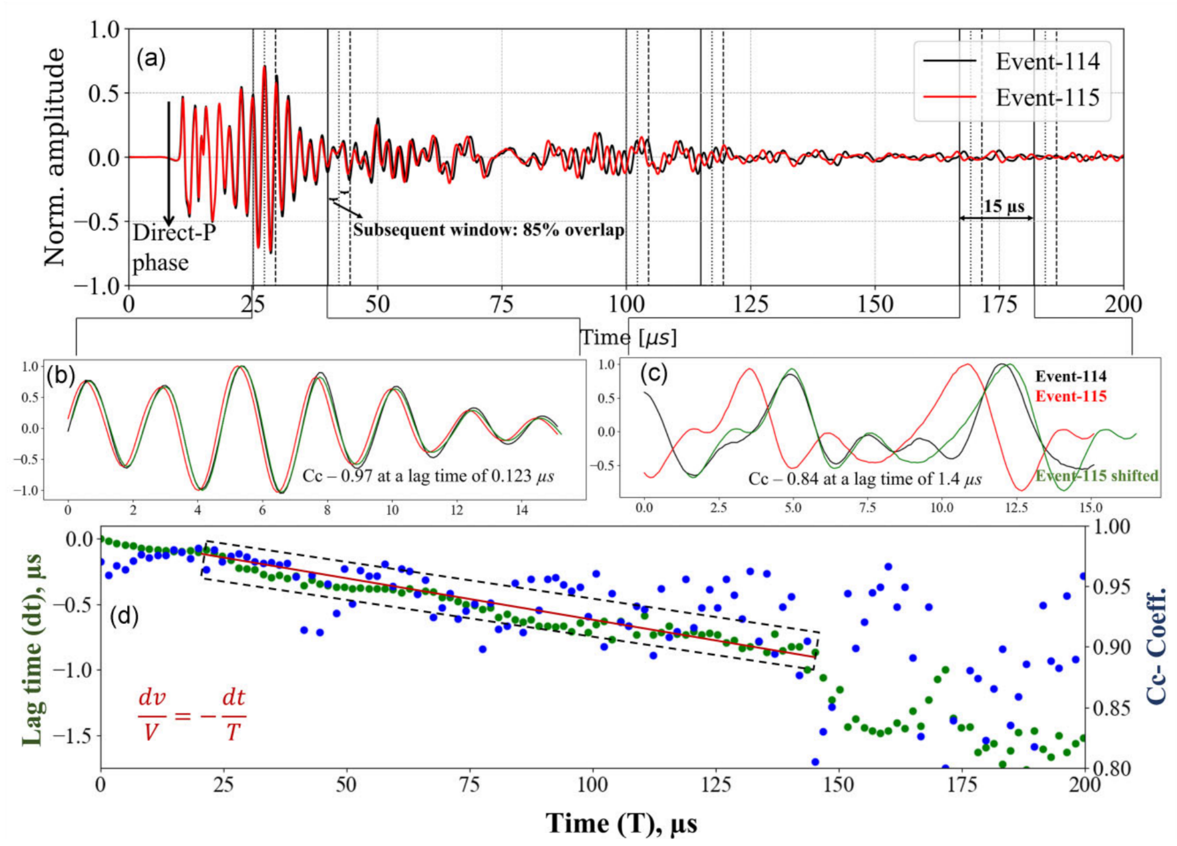

Figure 4: Two consecutive waveforms from a confining pressure increase experiment shows they are highly coherent. It also shows the 15 µs waveform window and an overlap of 85 per cent between two consecutive waveforms. The early part of the consecutive waveforms is highly coherent (b, c, d) with a very small lag. However , the later part has a very low cross-correlation value with a high associated lag. (d) Lag time over the length of the waveform shows the progression of the cross-correlation coefficient (blue) and the lag time (green) with the moving window cross-correlation method. The linear slope (ordinary least square fit) between 20 and 150 µs is considered for the dt/T, which is equivalent to −dv/V (relative seismic velocity change).

Anisotropic Microcrack

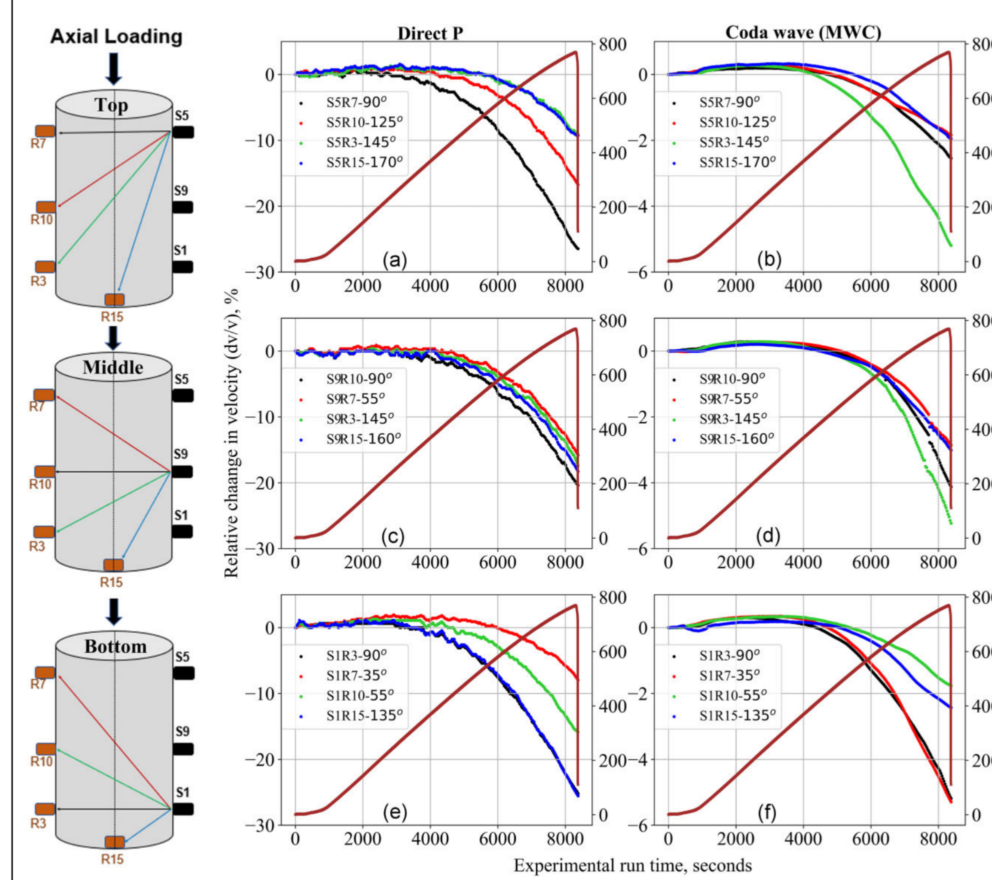

- We observe a pronounced seismic anisotropy due to preferential crack shapes and orientations. The seismic anisotropy increases after 335 MPa up to failure.
- As the experiment approaches failure, abundant wing cracks form with a preferred orientation sub-parallel to 1, leading to a higher level of anisotropy in the medium.
- We observe pronounced seismic anisotropy for the direct P wave; however, velocity estimates from CWI are not anisotropic but produce variations that are consistently more similar to the vertical direct P velocity.

Figure 5: Measurement of the relative change in velocity at different sections (top, middle and bottom) and along different ray paths (i.e. sensor–receiver orientations represented by red, green, black and blue color) for intact rock fracture experiment (Frac-1). a, c and e) Relative velocity change computed for direct P phase for different sender–receiver pairs. b, d and f) Change in velocity for coda wave computed from MWC method. Different colors correspond to different combinations of sender–receiver pairs or different ray paths. The brown curve represents the differential stress acting upon the sample. On the right, three cylinders show where the sender and receiver are at different sample parts.

Monitoring Preparatory Processes before Failure of Intact Rock Sample

Monitoring of Progressive Stress Accumulation through Seismic Velocity Changes

- Differential stress increase leading up to dynamic failure.
- **Phase I** is associated with initial crack closure, increasing velocity, and linear stress increase.
- **Phase II** marks the start of velocity decrease while stress increase remains linear.
- **Phase III** marks the onset of acoustic emission (AE) activity (colored by depth) which accelerates toward failure, deviation from linear stress increase, and a more rapid drop in seismic velocity.

Acoustic Emission (AE) Locations

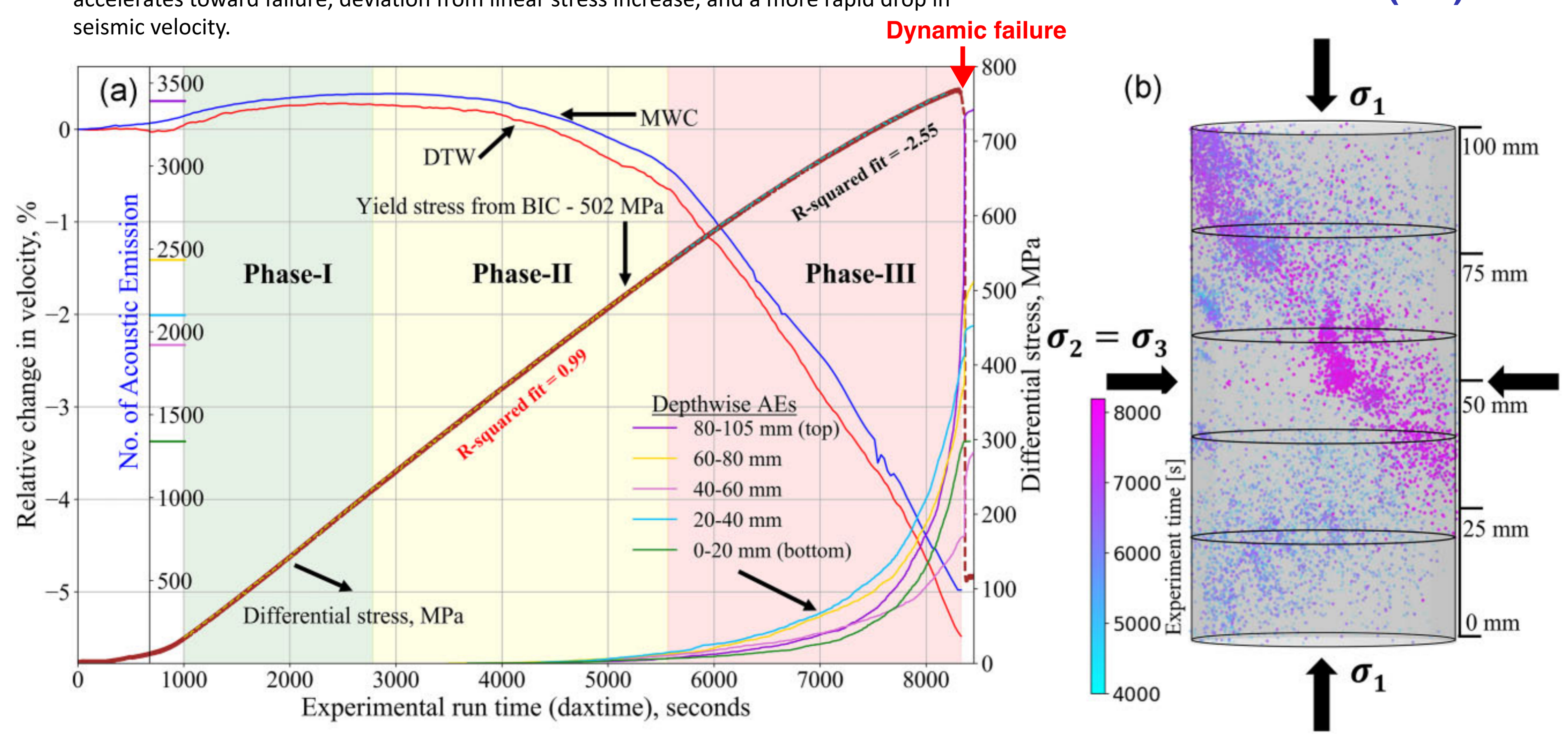

Figure 6: Microcrack compaction and creation can be separated into 3 phases based on average relative velocity changes in the horizontal direction (blue = moving window cross-correlation (MWC) and red = dynamic time warping (DTW)) and differential stress (black curve) for intact rock fracture experiment (Frac-1). Inset: Acoustic emission locations during early nucleation [blue: 6000 sec (582 MPa)–8000 sec (753MPa)], and fracture propagation (purple: 8000 + s). The horizontal lines between 3000 (260 MPa) and 4000 (371 MPa) sec display the maximum number of AEs for each depth distinguished by colors.

Crack Density Estimate

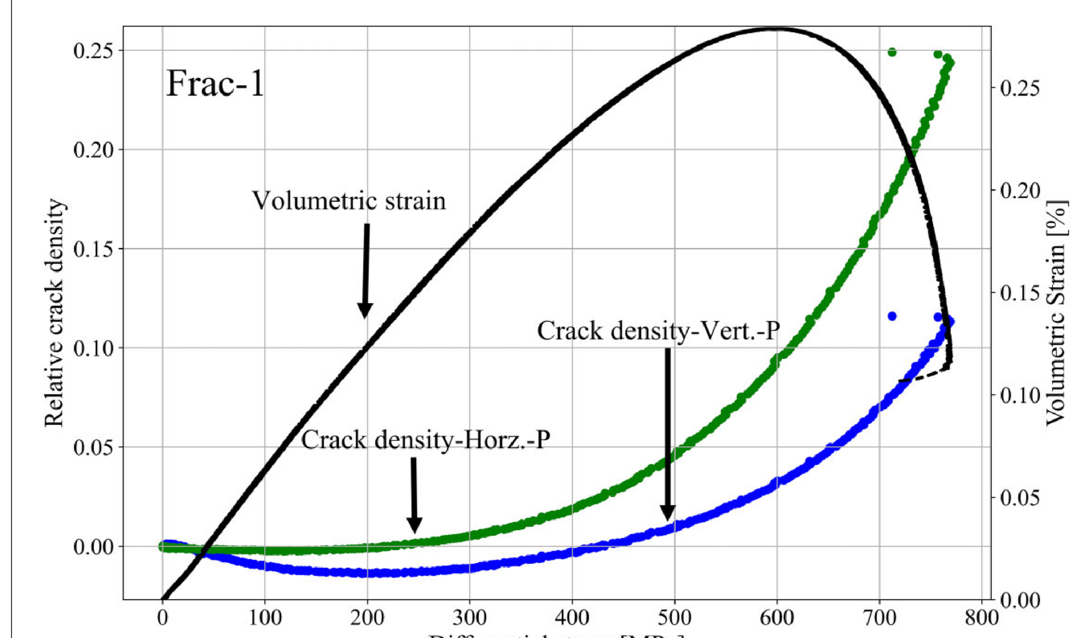

Figure 7: Comparison between the observed damage accumulation recorded by the strain gauges and crack density computed from the direct P-wave velocity. The plot of volumetric strain (black curve and right y -axis), and crack density from P-wave velocity (blue and green curves and left y -axis) plotted against differential stress for the intact rock fracture experiment (Frac-1).

- The seismic velocity estimates can detect changes in microcrack concentration before volumetric strain measurements can detect any significant changes.
- Crack densities inferred from velocity measurements indicate a short period of pore space reduction followed by a rapid increase in crack density towards failure.
- In contrast, the volumetric strain indicates macroscopic changes until much later into the loading cycle (i.e., until ≈ 500 MPa) when velocity-inferred crack density already indicates significant new micro-crack generation.

Fluid Injection Experiments

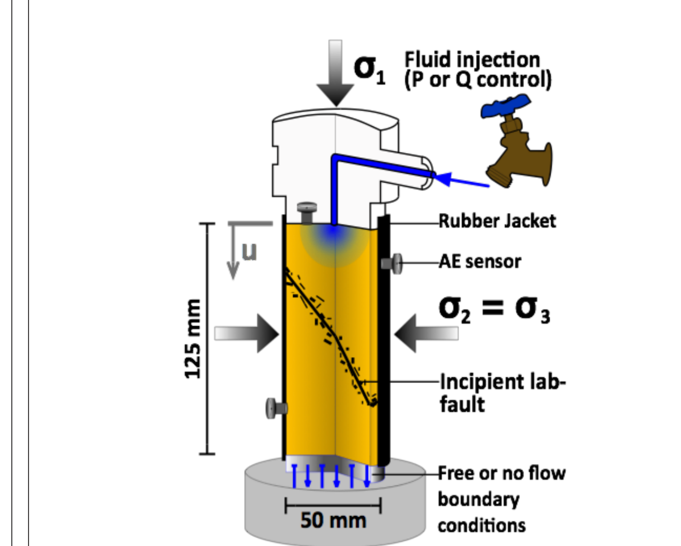

Figure 8: Overview of sample geometry and loading conditions. Fault creation and stick-slip occurs under triaxial loading conditions with servo-controlled axial load and confining pressure (σ1 > σ2 = σ3). Slip events are created by axial loading at constant pore-pressure or injecting fluids at stresses close to failure. Fluids can be injected through the end surfaces of the samples, resulting in a slow diffusive process or directly onto the fault through a central borehole.

Acknowledgments

- We thank the United States Geological Survey (G21AP10050 and G21AP10032) for their financial support. We also acknowledge the German Research Centre for Geosciences for providing us with the opportunity and facilities for the research.